RaDE: A Rank-based Graph Embedding Approach

Filipe Alves de Fernando, Daniel Carlos Guimarães Pedronette, Gustavo José de Sousa,
Lucas Pascotti Valem and Ivan Rizzo Guilherme

Institute of Geosciences and Exact Sciences, UNESP - São Paulo State University, Rio Claro, SP, Brazil

Keywords: RaDE, Graph Embedding, Network Representation Learning, Ranking.

Abstract: Due to possibility of capturing complex relationships existing between nodes, many application benefit of
being modeled with graphs. However, performance issues can be observed on large scale networks, making
it computationally unfeasible to process information in various scenarios. Graph Embedding methods are
usually used for finding low-dimensional vector representations for graphs, preserving its original properties
such as topological characteristics, affinity and shared neighborhood between nodes. In this way, retrieval
and machine learning techniques can be exploited to execute tasks such as classification, clustering, and link
prediction. In this work, we propose RaDE (Rank Diffusion Embedding), an efficient and effective approach
that considers rank-based graphs for learning a low-dimensional vector. The proposed approach was evaluated
on 7 network datasets such as a social, co-reference, textual and image networks, with different properties.
Vector representations generated with RaDE achieved effective results in visualization and retrieval tasks when
compared to vector representations generated by other recent related methods.

1   INTRODUCTION

In many real-world scenarios, the representation of
connections among elements is of crucial relevance.
In fact, it can be said that every entity in the universe
is connected with another in some aspect. Therefore,
with the prevalence of network data collected nowa-
days, from social media to communication or bio-
logical networks, learning and effectively represent-
ing such connections has become an essential task in
many applications (Huang et al., 2019).

Graphs are a natural way for representing entities
and connections. In such scenario, graphs assumed a
central role as an effective and powerful data repre-
sentation tool. Additionally, effective graph analysis
allow a deeper understanding of useful information
hidden behind the data. As a result, several important
applications can benefit from such analyses and have
their effectiveness improved, such as node classifica-
tion/retrieval, node recommendation, link prediction,
among others (Cai et al., 2018). Such wide range of
applications justifies the significant attention received
by graph-based approaches in the last decades (Huang
et al., 2019; Cai et al., 2018; Goyal and Ferrara,
2017).

Although graph analysis has emerged as an essen-
tial task, most of related methods requires high com-
putational costs (Cai et al., 2018). A promising solu-
tion consists in *graph embedding* approaches, which
have been increasingly exploited due to its capacity
of creating vector representations for nodes, edges or
even an entire network. Once graph structures can
be well represented into a vector space, many math-
ematical and machine learning tools can be utilized
for tasks such as classification, information retrieval,
clustering and so forth. Besides that, vector repre-
sentations generated by graph embedding methods
are able to compress huge networks into a significant
smaller amount of data while preserving most of orig-
inal information.

Graph embedding methods usually takes into ac-
count some of the structural aspects of the original
network for creating the embedding representation.
According to (Cai et al., 2018), the main goal of
graph embedding approaches is to represent a graph
as low dimensional vectors, while its structures are
preserved. As a result, high-effective graph embed-
ding methods are capable of keeping the accuracy of
retrieval and machine learning tasks, even when orig-
inal network had been significantly compressed. Ac-
tually, in some situations, the generated embedding
can even improve the accuracy in comparison to the
original graph representation.

In such scenario of crescent interest, various graph
embedding methods have been proposed in the last
years (Tang et al., 2015; Grover and Leskovec, 2016;

142

Wang et al., 2016; Ou et al., 2016). Most of them consider *node embedding* tasks, which also constitutes the main objective of this work. Also references in the literature (Cui et al., 2019) as Network Embedding or Network Representation Learning (NRL), such methods are usually used for finding low-dimensional vector representation for nodes, preserving its original properties such as topological characteristics, affinity and shared neighborhood between nodes. Different approaches focus on distinct aspects of embedding. The central idea of (Grover and Leskovec, 2016) consists in its flexible notion of a node's network neighborhood. On the other hand, the goal of preserving asymmetric transitivity is addressed by (Ou et al., 2016). First-order and second-order proximity are considered by (Wang et al., 2016) to preserve the network structure, while (Tang et al., 2015) focuses on large-scale datasets. Figure 1 illustrates a general scenario that different NRL methods can be applicable.

In this paper we present *RaDE*, a novel graph embedding algorithm for generating low-dimensional representations for nodes in networks. The proposed algorithm is completely unsupervised and defined through a ranked-based model. The central idea of our work consists in identifying high-effective representative nodes. In this way, each network node is represented according to its similarity to such representatives. Therefore, nodes with high-similarity to each other are expected to be also similar to same representatives. The representatives are selected based on the density of reciprocal similarity to its neighbors, which operates as an effectiveness estimation of representative rankings.

The main contributions and novelties of our proposed method are three-fold: (*i*) the ranked-based model used provides efficient structures for representing similarity information among nodes, which is innovative in graph embedding approaches; (*ii*) the proposed method requires no labeled data, based only on unsupervised estimations; (*iii*) the low computational costs, since the method is based only on ranking information and dispense costly optimization steps often involved in training steps.

A wide and comprehensive experimental evaluation was conducted to assess the effectiveness of generated embedding in retrieval tasks. The evaluation was conducted on 7 diverse datasets considering different data modalities: images, text, social networks, and a traditional pattern recognition dataset. Different networks, both dense and sparse, were also considered. The experimental results are compared with 4 recently proposed node embedding approaches. In various scenarios, the proposed method achieved best results in most of datasets, demonstrating the ability
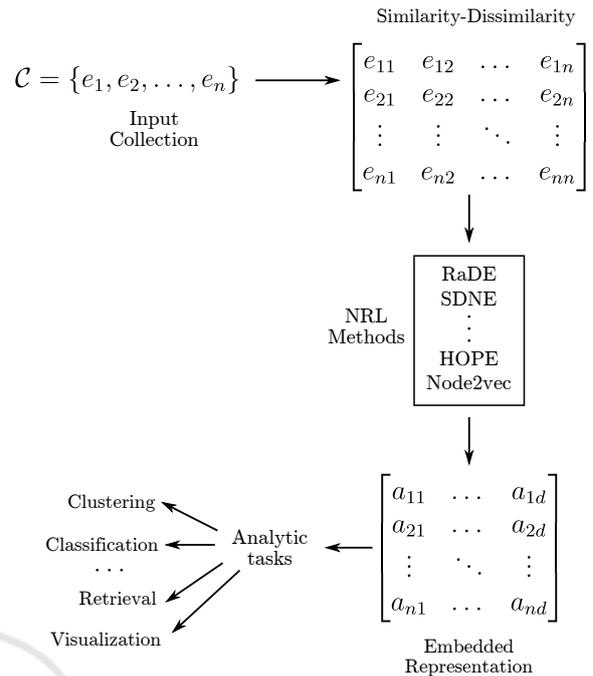

Figure 1: General scenario of application of NRL approaches.

in generating high-effective representations.

The remaining of this paper is organized as follows. Section 2 presents the formal definitions used along the paper. The proposed RaDE Node Embedding method is presented in Section 3. Section 4 discusses the experimental evaluation conducted. Finally, Section 5 discusses the conclusions and possible future work.

2 FORMAL PROBLEM DEFINITION

This section discusses a formal definition of the main task addressed in Section 2.1 and the rank model used in Section 2.2.

2.1 Graph Embedding

Let $\mathcal{C}=\{e_1, e_2, \ldots, e_n\}$ be a collection of data elements, where $n = |\mathcal{C}|$ denotes the size of $\mathcal{C}$. Along the paper, we relax the notation in such a way that an element $e \in \mathcal{C}$ can be used either as the element itself or its index, depending on context.

The collection $\mathcal{C}$ can be represented by a graph $G(V,E)$, where V is a set of vertices, such that $V = \mathcal{C}$, and $E \subseteq V^2$ is a set of edges. If $(e_i, e_j) \in E$, we say that vertices which represents elements e_i and e_j are connected in the graph. Weights can be assigned to

edges, commonly represented by an adjacency matrix $\mathbf{S}$ such that the value assigned to the edge (e_i, e_j) is given by $s_{i,j}$.

We define a *graph embedding* task (more specifically, *node embedding*) similarly to (Goyal and Ferrara, 2017). Given a graph $G(V,E)$, graph embedding can be seen as a mapping function $f : e_i \rightarrow \mathbf{v}_i \in \mathbb{R}^d$ $\forall i \in [n]$, such that the number of dimensions is much smaller than the collection size, i.e., $d \ll |V|$, and the function f preserves some structural information of the graph G. More specifically, it is expected that the similarity information encoded in the graph G is preserved, such that similar nodes in the graph are projected close in the $\mathbb{R}^d$ space.

2.2 Rank Model

As the proposed method is defined in terms of ranking information, this section presents a formal definition of the ranking model considered along the paper.

Let e_q be a query element. A ranked list τ_q can be computed in response to e_q, in which the top positions of τ_q are expected to contain the elements most similar to e_q. The ranking tasks are often defined through a pairwise dissimilarity measures, where the dissimilarity between two elements e_q and e_i is denoted by $\rho(q,i)$. As such, τ_q is sorted by the distances in ascending order, which means the full ranked list might be expensive to compute, specially when n is high. Therefore, the computed ranked lists can consider only a sub-set of the top-L elements.

Let τ_q be a ranked list that contains only the L elements most similar to e_q, where $L \ll n$. Formally, let C_L be a sub-set of C, such that $|C_L| = L$ and $\forall e \in C_L, e' \in C \setminus C_L, \rho(e_q, e) \leq \rho(e_q, e')$. The ranked list τ_q can then be defined as a bijection from the set C_L onto the set $[L] = \{1, 2, \dots, L\}$, such that $\forall e_i, e_j \in C, \tau_q(e_i) < \tau_q(e_j) \iff \rho(e_q, e_i) < \rho(e_q, e_j)$.

Every element $e_i \in C$ can be taken as a query element e_q. As a result, a set of ranked lists $\mathcal{T} = \{\tau_1, \tau_2, \dots, \tau_n\}$ can be obtained, with a ranked list for each element in the collection C. The set $\mathcal{T}$ constitutes a rich source of similarity information about the dataset. Such information is exploited to compute the embedding.

3 RaDE NODE EMBEDDING

Rank-based approaches have been successfully used in diverse retrieval and machine learning tasks recently (Zhong et al., 2017; Pedronette et al., 2019), mainly due to its capacity of encoding relevant similarity information defined in relationships among

dataset elements. Such capacity is exploited in this paper in order to embed the nodes from a similarity graph into a vector space, while maintaining similarity and neighborhood relationships. The used rank-based model allows an efficient similarity representation, since the most relevant information are located at top rank positions. In addition, the proposed method is completely unsupervised and data-independent.

Given a graph with edge weights assigned by similarity/dissimilarity measures, we derive an intermediary graph representation based only on ranking information. Next, our method exploits this graph to learn a novel vector representation based on two conjectures: (*i*) high-effective representative nodes can be identified by analysing the rank-based graph; (*ii*) each node can be represented according to its similarity to a set of representative nodes. In this way, the method can be computed through three main steps:

- A. Rank-based Similarity Graph:
- B. High-Effective Representative Nodes:
- C. Node Embedding:

Such steps are illustrated in Figure 2. Each step is detailed and formally defined in next sub-sections.

3.1 Rank-based Similarity Graph

Various retrieval and machine learning approaches define a similarity matrix $\mathbf{W}$ that represents a graph based on a dissimilarity measure ρ. A Gaussian kernel is often considered, such that $w_{ij} = exp(\frac{-\rho^2(i,j)}{2\sigma^2})$, where σ is a parameter to be defined.

Inspired by (Pedronette et al., 2019; Pedronette and da S. Torres, 2017), we define a rank similarity matrix $\mathbf{W}$ based only on rank information. The similarity score w_{ij} varies according to the position of e_j in the ranked list τ_i. Additionally, the score considers only a neighborhood set, which is limited by the size L of the ranked lists. Thus, the element w_{ij} of $\mathbf{W}$ is defined as:

$$w_{ij} = \begin{cases} 1 - \log_L \tau_i(e_j), & \text{if } \tau_i(e_j) \text{ is defined} \\ 0 & \text{otherwise.} \end{cases} \quad (1)$$

L can assume different values depending on the desired analysis. In the proposed method, the matrix $\mathbf{W}$ is defined assuming $L \ll n$ and, since it has dimension of $n \times n$, $\mathbf{W}$ is very sparse.

3.2 High-effective Representative Nodes

The proposed approach relies on determining the most representative nodes in a graph for generating an
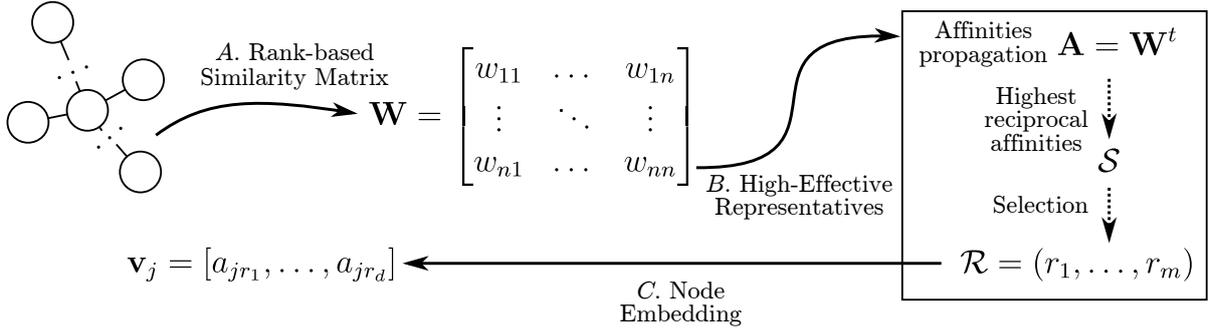
Figure 2: Main steps of the RaDE algorithm.

embedding representation. Our guiding hypothesis is that a good representative node has high affinity with nearest nodes and low affinity with distant nodes.

First, we compute contextual affinities, which take into account the structure of dataset manifold. The key idea is based on diffusion process methods (Donoser and Bischof, 2013; Bai et al., 2019), which propagate affinities encoded in $\mathbf{W}$. The more global similarity measures can be obtained by powers of $\mathbf{W}$, as shown in Equation 2:

$$\mathbf{A} = \mathbf{W}^t, \qquad (2)$$

where t is a constant that defines the number of iterations. A small value of $t = 2$ was used in all experiments.

Note that $\mathbf{A}$'s diagonal values represent reciprocal affinities. For example, for $t = 2$, $a_{ii} = \sum_{j=1}^{n} w_{ij}w_{ji}$, which means that d_{ii} aggregates direct reciprocal affinities between e_i and all the other elements. For $t > 2$, the diagonal still encodes reciprocal affinity, but indirectly.

We use the diagonal to find a set of k high-effective representative candidates, namely $\mathcal{S}$. The items in this set are supposed to satisfy the first requirement of our guiding hypothesis, thus this set is composed by the k elements with the highest reciprocal affinities. Elements with high reciprocal similarities are expected to have high-effective ranked lists, and therefore be good candidates.

Formally, the candidates set $\mathcal{S}$ must hold the following properties:

$$\mathcal{S} \subseteq \mathcal{C} \qquad (3)$$
$$|\mathcal{S}| = k \qquad (4)$$
$$\forall e \in \mathcal{S}, e' \in \mathcal{C} \setminus \mathcal{S}, a_{ee} \geq a_{e'e'} \qquad (5)$$

Finally, a resulting ordered list of d representative nodes is obtained from the set of candidates $\mathcal{S}$. The objective is to select high-effective candidates with the maximum of diversity among them. In this way, both the diagonal affinity scores and the affinities to already selected nodes are considered. Let

$\mathcal{R} = (r_1, r_2, \ldots, r_d)$ be an ordered list with the d most effective representative nodes, each element r_i is defined as:

$$r_i = \arg\max_{e \in \mathcal{S} \setminus \mathcal{R}_{i-1}} \frac{a_{ee}}{1 + \sum_{j=1}^{i-1} a_{er_j}}, \qquad (6)$$

where $\mathcal{R}_{i-1} = \{r_1, \ldots, r_{i-1}\}$ is the set of the elements selected for previous indexes.

The main objective of Equation 6 is to complete our guiding hypothesis, by favoring elements with high reciprocal affinity, but, at the same time, penalizing them for being similar to the ones already selected.

3.3 Node Embedding

Once the representative nodes have been chosen, the embedding can be generated for any desired data element. The embedding is computed based on the conjecture that nodes similar to each other are also similar to the same set of representative nodes. Formally, the embedded vector $\mathbf{v}_j$ for an element $e_j \in \mathcal{C}$ is defined as follows:

$$\mathbf{v}_j = [a_{jr_1}, \ldots, a_{jr_d}], \qquad (7)$$

where a_{jr_i} denotes the affinity between the the element e_j and the representative node r_i.

4 EXPERIMENTAL EVALUATION

A broad experimental analysis was conducted to evaluate the proposed method. An overview about experiments is discussed in Section 4.1. Section 4.2 presents the datasets, while Section 4.3 describes the baselines. Section 4.4 and 4.5 discusses the evaluation measures and parameters settings, respectively. The results on diverse information retrieval tasks are discussed in Section 4.6. A visual analysis is presented in Section 4.7.

4.1 Overview of Experiments

The vector representations generated with RaDE were evaluated on information retrieval and visualization tasks on 7 datasets of multiple domains (e.g. images, texts and social networks) and each of these datasets have different characteristics (e.g. dense or sparse graphs, weighted or not weighted graphs, large or low scale graphs).

The datasets of images and texts are not networks by itself. In order to be able to apply Network Representation Learning methods on these datasets, it is necessary to generate a graph from the original dataset. For this task, two main steps are necessary: *i)* extracting the feature vectors of samples in dataset; *ii)* calculating distances between the extracted features for generating a graph weighted by these distances. In this work the graphs generated for this kind of dataset were complete[1] and the Euclidean distance was used to calculate the weights.

Other category of datasets used to evaluate the proposed approach was datasets that are networks by itself. The selected network datasets are not originally weighted and for being able to apply RaDE, the datasets must be weighted. For doing that we used an approach based on shared neighborhood between nodes.

The vector representations generated by RaDE were compared with the vector representations generated by 4 other Network Representation Learning methods which have characteristics different from each other. The implementation provided by OpenNE library [2] was used for executing the experiments and they were executed on a machine with a Intel Xeon E5-2660 @ 2.0Ghz processor, 64GB of RAM and Arch Linux x86_64, kernel version 5.0.7 OS.

4.2 Datasets

We evaluated the effectiveness of RaDE on 7 datasets of multiple domains. MPEG-7 (Latecki et al., 2000), Oxford17Flowers (Nilsback and Zisserman, 2006) and Corel5k (Liu et al., 2010) are image datasets where each sample is described in function of its extracted features. The features for Oxford17Flowers (Nilsback and Zisserman, 2006) and Corel5k (Liu et al., 2010) were extracted using the descriptors that presented the highest MAP according to experimental results presented on (Valem and Pedronette, 2019). For MPEG-7 (Latecki et al., 2000), the features were

extracted using a contour descriptor (Pedronette and da Silva Torres, 2010).

The weighted graphs, for MPEG-7 (Latecki et al., 2000), Oxford17Flowers (Nilsback and Zisserman, 2006), Corel5k (Liu et al., 2010), 20NewsGroup (Lang, 1995) and Iris (Dua and Graff, 2017), were generated using the Euclidean distances between features vector of each sample. For datasets that originally are networks, such as BlogCatalog (Zafarani and Liu, 2009) and Wiki [3], it was necessary an strategy for assigning the weights, since they are not originally weighted. We assumed that the more neighbors are shared between a pair of nodes, the more similar they are to each other. The approach used for assigning the weights is described in Equation 8,

$$w_{i,j} = \frac{1}{1 + \mathcal{N}(i,m) \cap \mathcal{N}(j,m)}, \qquad (8)$$

where $\mathcal{N}(i,m)$ is the m nearest neighbors of a node N_i.

The details about each dataset evaluated on this work are exposed bellow:

- MPEG-7 (Latecki et al., 2000): 1,400 images, divided into 70 balanced classes, each one containing 20 samples. The features of the images were extracted by CFD (Pedronette and da Silva Torres, 2010) which is a contour based descriptor.

- Oxford17Flowers (Nilsback and Zisserman, 2006): 1,360 images of 17 different species of flowers, each one containing 80 different images. Each image is described in function of 2,048 features, which were extracted using ResNet152 [4] which is a residual neural network pre-trained on ImageNet Dataset (Deng et al., 2009).

- Corel5k (Liu et al., 2010): 5,000 miscellaneous images (e.g. fireworks, trees, boats, tiles, etc). This dataset is divided into 50 categories, with 100 images each. Each image is described in function of 1,000 features, which were extracted using a DualPathNetwork92 [5].

- Iris (Dua and Graff, 2017): A dataset widely used in pattern recognition task. It contains 150 samples of flowers, divided into 3 balanced classes. Each sample is described in function of the petal and sepal width and petal and sepal length.

- BlogCatalog3 (Zafarani and Liu, 2009): A social network that contains 10,312 nodes and 333,983 edges. Each node represents a blogger and each

---

[1]Note, however, that the proposed method does not require the graph to be complete.

[2]https://github.com/thunlp/OpenNE

[3]https://github.com/thunlp/OpenNE

[4]https://github.com/Cadene/pretrained-models.pytorch

[5]https://github.com/Cadene/pretrained-models.pytorch

edge represents the friendships between two bloggers. The nodes are separated into 39 groups and each blogger may belong to more than one group.

- Wiki [6]: A reference network between Wikipedia documents. It contains 2,405 documents divided into 19 classes. This network is composed by 17,981 edges, it is not originally weighted and it is directed.

- 20NewsGroup (Lang, 1995): Originally, it contains 18,846 news texts, sorted by date and separated into 20 categories. In this work, we choose only 3 categories (*comp.graphics*, *rec.sport.baseball* and *talk.politics.gums*) that compose a subset with 1,729 texts, similarly to what was done in (Wang et al., 2016). The features of each document were extracted based on its respective TF-IDF (Salton and Buckley, 1988) vector.

4.3 Baseline Algorithms

The vector representations generated by RaDE were compared with the following algorithms:

- Node2vec (Grover and Leskovec, 2016) aims to learn low dimensional vector representation for nodes in a network by generating random walks starting from each of them. Node2vec is a generalization Deep Walk (Perozzi et al., 2014) that introduces two parameters responsible for generating biased random walks, preserving properties either of the local community or the global structure of the network.

- HOPE (Higher Order Proximity Embedding) (Ou et al., 2016) is a scalable node embedding approach. HOPE aims to preserve asymmetric transitivity, which is a property existing on directed graphs that depicts correlation between directed edges and can help in capturing and recovering the structure of a network from partially observed graph.

- LINE (Large Scale Information Network Embedding) (Tang et al., 2015) is a scalable approach able to learn low dimensional vector representations of nodes from networks with millions of nodes and billions of edges in a few hours. This method defines an objective function that aims to preserve two main properties of nodes: first order proximity and second order proximity. First order proximity is directly proportional to the connection power between a pair of nodes and second

---

[6]https://github.com/thunlp/OpenNE

order proximity is direct proportional to the number of direct neighbors shared between a pair of nodes.

- SDNE (Structural Deep Network Embedding) (Wang et al., 2016) proposes a deep model capable of capturing highly non-linear network structure and extends the traditional autoencoder architecture to preserve both the first order and second order proximity of networks.

4.4 Evaluation Measures

The results were reported considering two different effectiveness measures commonly used for information retrieval tasks: Precision and Mean Average Precision (MAP). Given a ranked list τ_q as input, the measures report a score in the interval $[0, 1]$, where higher values refer to better results. The results correspond to the mean of these measures computed for each of the ranked lists in the dataset.

4.4.1 Precision

The Precision measure corresponds to the number of retrieved samples that belong to the class of the query element in the top-k positions. This is formally defined by Equation 9.

$$P(q,k) = \frac{1}{k} \times \sum_{i=1}^{k} f_c(\tau_q^{-1}(i), q), \qquad (9)$$

where q is the index of the query element, k is the size of the ranked list, $\tau_q^{-1}(i)$ is the i-th element in the ranked list and f_c is a function that returns 1 if two elements belong to the same class and 0 otherwise. In this case, it is equivalent to the number of true positives against the sum of true positives and false positives. For readability purposes, to report the mean of the Precision of all elements, we use P@k.

4.4.2 Mean Average Precision (MAP)

The Average Precision (A_p) computes the sum of the Precisions for different depths of a ranked list, which is formally defined in Equation 10.

$$A_p(q,k) = \frac{1}{f_s(q)} \times \sum_{i=1}^{k} P(q,i) \times f_c(\tau_q^{-1}(i), q), \quad (10)$$

where q is the index of the query element, k is the depth of the ranked list, f_s is a function that returns the class size of an element, $\tau_q^{-1}(i)$ is the i-th element in the ranked list and f_c is a function that returns 1 if two elements belong to the same class and 0 otherwise.

The MAP (Mean Average Precision) is defined as the mean of A_p for all the Q queries. The formulation is given by Equation 11.

$$MAP = \frac{\sum_{q=1}^{Q} A_p(q)}{Q} \qquad (11)$$

4.5 Parameter Settings

For information retrieval task, the generated vector representations were composed by 128 dimensions, while for visualization task they were composed by 100 dimensions.

Table 1 shows the parameter settings for each method. Most of methods was executed with the default parameter configuration, provided by the OpenNE library.

Table 1: Parameter settings for each evaluated method.

Method	Parameters
Node2vec	**Number of paths:** 10 **Path length:** 80 **Window size:** 10 **p:** 0,25 **q:** 0,25
LINE	**Negative ratio:** 5 First and second order
SDNE	**Autoencoder List:** [1000, 128] **Learning rate:** 0,01 **First order loss:** 10^{-6} **l1 loss :** 10^{-5} **l2 loss:** 10^{-6} **Batch size:** 200
HOPE	—
RaDE	**t:** 2 **k:** 200 **L:** 25

4.6 Information Retrieval Results

In this section we present the results of RaDE on information retrieval task. The results were divided into two categories, according to the characteristics of evaluated networks. These categories are: dense networks and sparse networks.

4.6.1 Dense Networks

Dense networks are complete and directed. These networks were generated by extracting feature vectors from samples of the original dataset and these vectors were used to calculate the weights between each node.

The column "Original" refers to the Precision and MAP evaluation for the original weights, that is, be-

fore previous application of NRL methods. The number of dimensions of original vectors is equal to the number of nodes on the network, while vectors generated with NRL methods have 128 dimensions.

Once Node2vec is very expensive, vector representations with this method was generated only for networks which have less than 1,500,000 edges, except on 20NewsGroup dataset. Even being bigger than the restriction imposed, we presented the quantitative results for Node2vec on 20NewsGroup dataset because this dataset was evaluated on visualization task, and for the completeness sake, we had to calculate vector representations for each method. However, the embeddings of Node2vec presented on 20NewsGroup are different than others because it has only 100 dimensions instead of 128 dimensions.

Table 2: 20NewsGroup evaluation.

	Original	RaDE	HOPE	LINE	SDNE	Node2vec
P@2	0.9690	**0.9574**	0.9253	0.6621	0.7292	0.6693
P@4	0.9337	**0.9208**	0.8824	0.4994	0.5791	0.4998
P@8	0.8841	**0.8878**	0.8523	0.4108	0.4932	0.4162
P@16	0.8318	**0.8473**	0.8256	0.3691	0.4551	0.3753
P@32	0.7713	**0.7973**	0.7937	0.3488	0.4352	0.3543
P@64	0.6965	*0.7219*	**0.7479**	0.3418	0.4242	0.3445
P@128	0.6076	*0.6177*	**0.6765**	0.3381	0.4166	0.3399
MAP	0.4924	*0.4513*	**0.5132**	0.3396	0.4051	0.3404

Table 3: Iris evaluation.

	Original	RaDE	HOPE	LINE	SDNE	Node2vec
P@2	0.9800	**0.9933**	0.9833	0.9366	0.99	0.9233
P@4	0.9633	**0.9700**	0.9650	0.8550	0.9616	0.8850
P@8	0.9500	*0.9466*	**0.9533**	0.8008	0.9233	0.8616
P@16	0.9337	*0.9295*	**0.9362**	0.7591	0.8791	0.8370
P@32	0.8947	*0.8725*	**0.8937**	0.7068	0.8410	0.8029
P@64	0.7002	*0.6879*	**0.7043**	0.5871	0.6720	0.6666
P@128	0.3904	*0.3884*	**0.3906**	0.3871	0.3875	0.3899
MAP	0.8858	*0.8688*	**0.8905**	0.6988	0.8400	0.8082

HOPE achieved the best MAP results on 20NewsGroup and Iris as presented on Table 2 and Table 3, respectively. Meanwhile, RaDE achieved the second best result for both precision and MAP on these datasets besides achieving the best Precision results on first positions, which is desirable for information retrieval task.

Our approach was able to create vector representations 13.50 times smaller than the originals with only 8.34% of relative MAP loss on 20NewsGroup. Besides that, RaDE improved the Precision of the original vector representations for $k \geq 8$ on this 20NewsGroup.

For the three images datasets evaluated shown on Table 4, Table 5 and Table 6, RaDE presented the highest MAP compared with the baseline methods. Our approach improved the relative MAP to the original vector representations by 9.08% on the MPEG-7, 16.32% on Flowers and 1.68% on Corel5k. These

Table 4: MPEG-7 evaluation.

	Original	RaDE	HOPE	LINE	SDNE
P@2	0.9921	*0.9668*	**0.9871**	0.8892	0.6146
P@4	0.9786	*0.9239*	**0.9560**	0.7889	0.4019
P@8	0.9320	*0.8749*	**0.9023**	0.6800	0.2716
P@16	0.8212	**0.8192**	0.8143	0.5735	0.1894
P@32	0.5125	**0.5174**	0.5144	0.3810	0.1369
P@64	0.2760	**0.2717**	0.2751	0.2226	0.0990
P@128	0.1448	*0.1399*	**0.1442**	0.1266	0.0720
MAP	0.8071	**0.8804**	0.8008	0.5565	0.1860

Table 5: Flowers evaluation.

	Original	RaDE	HOPE	LINE	SDNE
P@2	0.9401	**0.9276**	0.9047	0.7772	0.6117
P@4	0.8906	**0.8779**	0.8292	0.6250	0.3641
P@8	0.8349	**0.8385**	0.7638	0.5245	0.2382
P@16	0.7707	**0.8043**	0.6926	0.4596	0.1652
P@32	0.6800	**0.7484**	0.6072	0.3976	0.1280
P@64	0.5488	**0.6347**	0.4856	0.3314	0.1060
P@128	0.3713	**0.4057**	0.3373	0.2555	0.0963
MAP	0.5183	**0.6029**	0.4466	0.2930	0.1115

Table 6: Corel5k evaluation.

	Original	RaDE	HOPE	LINE	SDNE
P@2	0.9621	**0.9430**	0.7867	0.6144	0.5160
P@4	0.9290	**0.9070**	0.6622	0.4140	0.2742
P@8	0.8988	**0.8795**	0.5894	0.3026	0.1518
P@16	0.8595	**0.8541**	0.5377	0.2358	0.0894
P@32	0.8070	**0.8176**	0.4931	0.1930	0.0581
P@64	0.7206	**0.7503**	0.4372	0.1584	0.0422
P@128	0.5232	**0.5402**	0.3211	0.1253	0.0339
MAP	0.6517	**0.6627**	0.3100	0.1043	0.0375

improvements were achieved with vector representations 10.94, 10.63 and 39.06 times smaller respectively.

For both, Flowers and Corel5k, RaDE outperformed the baselines on Precision evaluation for highest k. On these datasets, for lower k, the Original vector representation presented the best precision results. However, as shown on Table 5 and on Table 6, when $k \geq 8$ and $k \geq 32$, RaDE overcame the Original vector representation for Flowers and Corel5k respectively.

Although RaDE did not have shown the best precision results for MPEG-7, our approach presented very close results to Original vector representation, which presented the best performance for this dataset.

4.6.2 Sparse Networks

These datasets are characterized by being networks by itself and are sparse, undirected and unweighted. Since RaDE is only applicable for weighted graphs, we used an approach for assigning the weights be-

Table 7: BlogCatalog evaluation.

	RaDE	HOPE	LINE	SDNE	Node2vec
P@2	*0.5724*	0.5950	0.6287	0.5565	**0.6692**
P@4	*0.3553*	0.3844	0.4358	0.3337	**0.4831**
P@8	*0.2415*	0.2741	0.3315	0.2200	**0.3755**
P@16	*0.1807*	0.2140	0.2731	0.1620	**0.3065**
P@32	*0.1472*	0.1801	0.2371	0.1309	**0.2607**
P@64	*0.1272*	0.1598	0.2109	0.1139	**0.2278**
P@128	*0.1156*	0.1461	0.1887	0.1043	**0.2006**
MAP	*0.0918*	0.1033	0.1227	0.0928	**0.1300**

Table 8: Wiki evaluation.

	RaDE	HOPE	LINE	SDNE	Node2vec
P@2	*0.7748*	0.7848	**0.8299**	0.8008	0.8168
P@4	*0.6419*	0.6511	**0.7059**	0.6740	0.6936
P@8	*0.5525*	0.5634	**0.6061**	0.5696	0.6001
P@16	*0.4882*	0.4836	0.5108	0.4666	**0.5175**
P@32	*0.4294*	0.4027	0.4198	0.3649	**0.4484**
P@64	*0.3677*	0.3103	0.3317	0.2720	**0.3756**
P@128	*0.2838*	0.2233	0.2489	0.2021	**0.2933**
MAP	*0.2438*	0.1971	0.2317	0.1833	**0.2554**

tween nodes based on the shared neighborhood, as described in Equation 8.

For the evaluated sparse networks, the best results were achieved by Node2vec. Table 7 shows a relative loss by 29.4% between Node2vec and RaDE on Blog-Catalog and Table 8 shows a relative loss by 4.55% on Wiki for these methods. Despite RaDE did not performed well on BlogCatalog, our approach outperformed the results of MAP and Precision for $k \geq 16$ on Wiki, of the baselines except Node2Vec.

A possible reason for RaDE did not have performed well on BlogCatalog may be due to the weighting strategy used. We plan in the future to evaluate other sparse networks already weighted as well as to investigate different weighting strategies for the unweighted ones.

4.7 Visualization Tasks

Vector representations generated with RaDE were also evaluated on visualization tasks. On this experiment, we evaluated the effectiveness of vector representations generated by the baselines presented on Subsection 4.3 on two datasets: Iris and 20NewsGroup. We used these datasets due to the fact that they are composed by only 3 classes, therefore they are good candidates for visualization tasks.

We generated new vector representations for 20NewsGroup and Iris with each NRL algorithm described on Subsection 4.3. The vector representations were generated with 100 dimensions, except to the original vector representations, which have 150 and
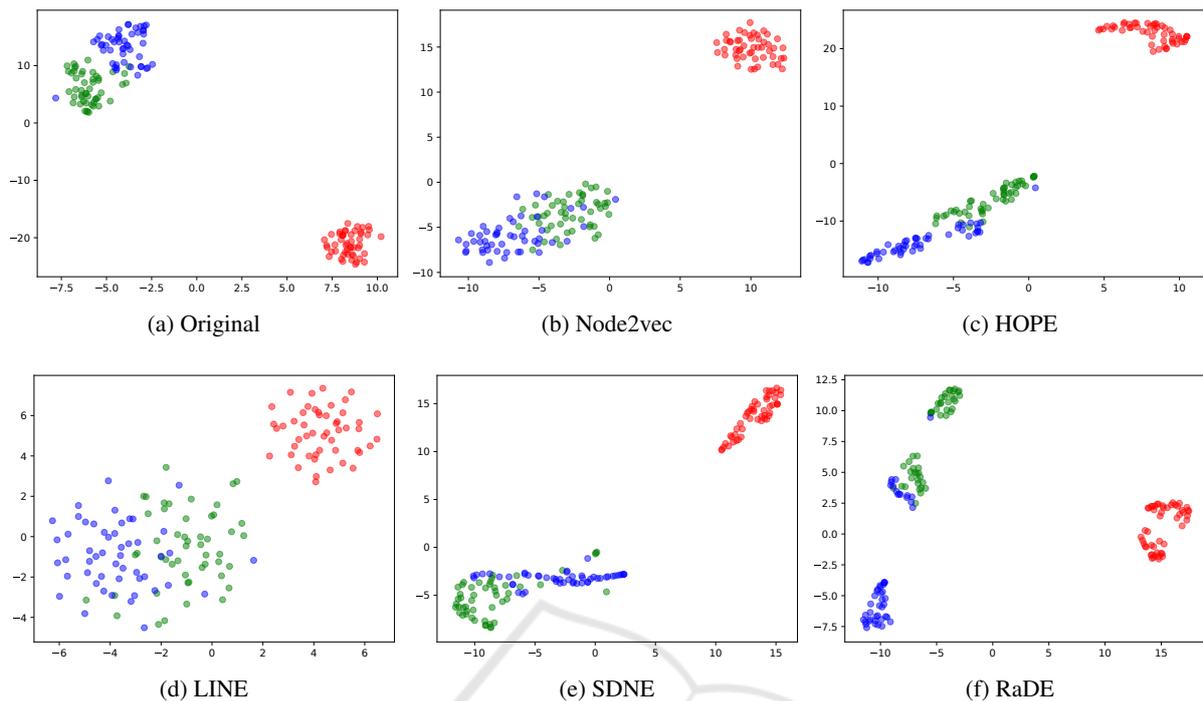
Figure 3: Visual Evaluation on Iris.

1,729 dimensions for Iris and 20NewsGroup, respectively. Then, we used these embeddings as input for t-SNE (van der Maaten and Hinton, 2008) in order to generate the visualization. It is common to perform a dimensionality reduction of the data using methods like (Jolliffe and Springer-Verlag, 2002) before generating the visualization with t-SNE. The step of generating the 100-dimensional embeddings with the NRL algorithms is analogous to this pre-processing step of t-SNE.

As shown on Figure 3, t-SNE separated well the red class, which is linearly separable from the others. The Original vector representation and vector representations generated by HOPE and RaDE presented the best visual results on Iris, being consistent with the quantitative results presented on Table 3.

Another interesting result that can be observed on Figure 3 is the fact that RaDE created well defined clusters for samples that are known to belong to different classes. Note that blue samples are grouped on the bottom and green samples are grouped on the top of Figure 3 (f). Between these clusters, RaDE created another cluster that contains samples which do not have the same degree of assurance of belonging to a class as the others well clustered. There are plans to investigate the reason for this behaviour in future works.

As well as results observed for the Iris dataset on Figure 3, the best visual results from 20NewsGroup,

were given by the Original, HOPE and RaDE vector representations, as shown on Figure 4. Even reducing the amount of information needed to represent the original data, vectors generated by HOPE and RaDE resulted on more interesting visual representations than Node2vec, LINE and SDNE. Visual results presented on Figure 4 shown that red samples was separated better with RaDE than HOPE.

5 CONCLUSION

In this work, we introduced RaDE, an unsupervised method for generating low-dimensional vector representations based on similarity between common nodes and high-effective representative nodes in a network. RaDE has achieved the best results in most of the evaluated datasets, specially on the evaluated image datasets, which are dense networks. Our approach was capable of creating high-effective low-dimensional vector representations that can be useful in many tasks such as information retrieval and visualization. In the most cases, RaDE was not only capable of providing very dense and smaller representations, but has also improved the general effectiveness by a significant margin. For the Corel5k dataset, for example, the provided output is 39.06 times smaller than the original vector and +1.68% more effective when considering the relative gain of the MAP. Gains
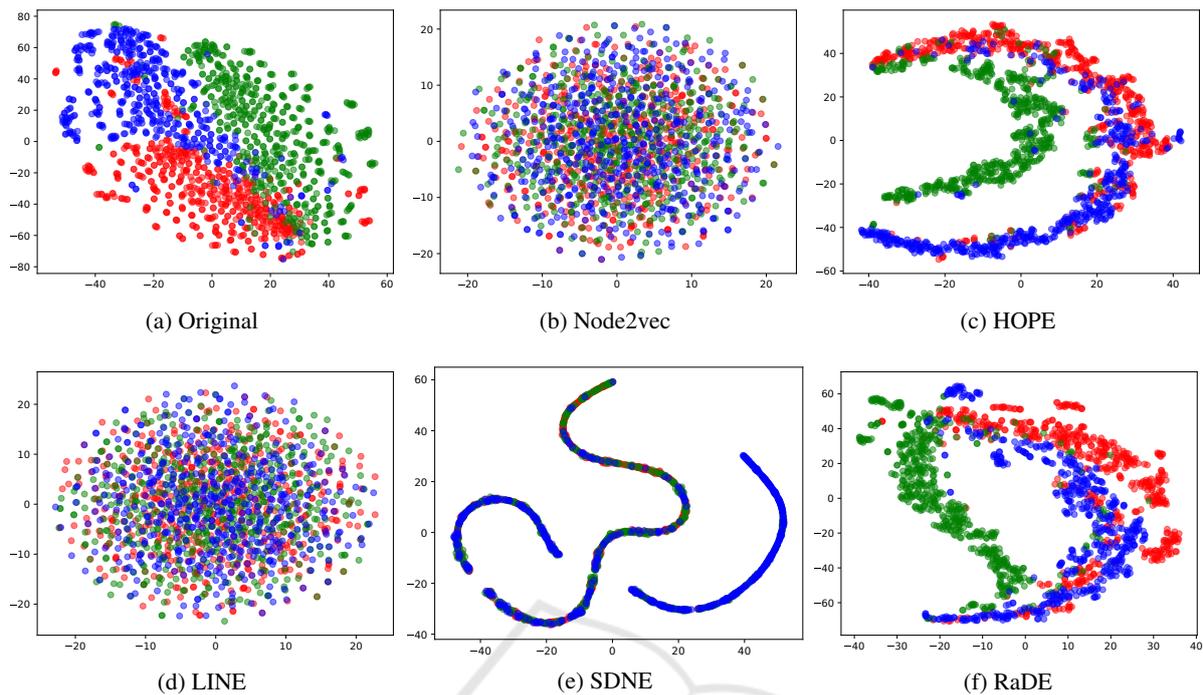
Figure 4: Visual Evaluation on 20NewsGroup.

were also achieved for other datasets, including Flowers, where the MAP improvement of features is up to +16.32% even with a reduction of 10.63 times of the original size. Therefore, RaDE demonstrated to be an interesting approach to reduce the dimensionality of dense networks preserving its original meaning.

For future works, we plan to investigate what makes RaDE provide more effective clusters when compared to baselines, as observed in the visualization result on Iris dataset. We also intend to perform a strict parameter analysis for both RaDE and baselines. Besides that, we plan to optimise the implementation of RaDE, in order to perform efficiency analyzes.

ACKNOWLEDGEMENTS

REFERENCES

Bai, S., Bai, X., Tian, Q., and Latecki, L. J. (2019). Regularized diffusion process on bidirectional context for object retrieval. *IEEE Trans. Pattern Anal. Mach. Intell.*, 41(5):1213–1226.

Cai, H., Zheng, V. W., and Chang, K. C. (2018). A comprehensive survey of graph embedding: Problems, techniques, and applications. *IEEE Trans. Knowl. Data Eng.*, 30(9):1616–1637.

Cui, P., Wang, X., Pei, J., and Zhu, W. (2019). A survey on network embedding. *IEEE Transactions on Knowledge and Data Engineering*, 31(5):833–852.

Deng, J., Dong, W., Socher, R., Li, L.-J., Li, K., and Fei-Fei, L. (2009). Imagenet: A large-scale hierarchical image database. In *2009 IEEE conference on computer vision and pattern recognition*, pages 248–255. Ieee.

Donoser, M. and Bischof, H. (2013). Diffusion processes for retrieval revisited. In *IEEE Conference on Computer Vision and Pattern Recognition, CVPR*, pages 1320–1327.

Dua, D. and Graff, C. (2017). UCI machine learning repository.

Goyal, P. and Ferrara, E. (2017). Graph embedding techniques, applications, and performance: A survey. *CoRR*, abs/1705.02801.

Grover, A. and Leskovec, J. (2016). Node2vec: Scalable feature learning for networks. In *Proceedings of the 22Nd ACM SIGKDD International Conference on Knowledge Discovery and Data Mining*, KDD '16, pages 855–864, New York, NY, USA. ACM.

Huang, X., Cui, P., Dong, Y., Li, J., Liu, H., Pei, J., Song, L., Tang, J., Wang, F., Yang, H., and Zhu, W. (2019). Learning from networks: Algorithms, theory, and applications. In *Proceedings of the 25th ACM SIGKDD*

International Conference on Knowledge Discovery & Data Mining, KDD '19, pages 3221–3222.

Jolliffe, I. and Springer-Verlag (2002). *Principal Component Analysis*. Springer Series in Statistics. Springer.

Lang, K. (1995). Newsweeder: Learning to filter netnews. In *Proceedings of the Twelfth International Conference on Machine Learning*, pages 331–339.

Latecki, L. J., Lakämper, R., and Eckhardt, U. (2000). Shape descriptors for non-rigid shapes with a single closed contour. In *Proc. IEEE Conf. Computer Vision and Pattern Recognition*, pages 424–429.

Liu, G.-H., Zhang, L., Hou, Y.-K., Li, Z.-Y., and Yang, J.-Y. (2010). Image retrieval based on multi-texton histogram. *Pattern Recogn.*, 43(7):2380–2389.

Nilsback, M.-E. and Zisserman, A. (2006). A visual vocabulary for flower classification. In *Proceedings of the 2006 IEEE Computer Society Conference on Computer Vision and Pattern Recognition - Volume 2*, CVPR '06, pages 1447–1454, Washington, DC, USA. IEEE Computer Society.

Ou, M., Cui, P., Pei, J., Zhang, Z., and Zhu, W. (2016). Asymmetric transitivity preserving graph embedding. In *Proceedings of the 22Nd ACM SIGKDD International Conference on Knowledge Discovery and Data Mining*, KDD '16, pages 1105–1114, New York, NY, USA. ACM.

Pedronette, D. C. G. and da S. Torres, R. (2017). Unsupervised rank diffusion for content-based image retrieval. *Neurocomputing*, 260:478 – 489.

Pedronette, D. C. G. and da Silva Torres, R. (2010). Shape retrieval using contour features and distance optimization. In *VISAPP (2)*, pages 197–202.

Pedronette, D. C. G., Valem, L. P., Almeida, J., and da S. Torres, R. (2019). Multimedia retrieval through unsupervised hypergraph-based manifold ranking. *IEEE Transactions on Image Processing*, 28(12):5824–5838.

Perozzi, B., Al-Rfou, R., and Skiena, S. (2014). Deepwalk: Online learning of social representations. In *Proceedings of the 20th ACM SIGKDD International Conference on Knowledge Discovery and Data Mining*, KDD '14, pages 701–710, New York, NY, USA. ACM.

Salton, G. and Buckley, C. (1988). Term-weighting approaches in automatic text retrieval. *Inf. Process. Manage.*, 24(5):513–523.

Tang, J., Qu, M., Wang, M., Zhang, M., Yan, J., and Mei, Q. (2015). Line: Large-scale information network embedding. In *Proceedings of the 24th International Conference on World Wide Web*, WWW '15, pages 1067–1077, Republic and Canton of Geneva, Switzerland. International World Wide Web Conferences Steering Committee.

Valem, L. P. and Pedronette, D. C. G. a. (2019). An unsupervised genetic algorithm framework for rank selection and fusion on image retrieval. In *Proceedings of the 2019 on International Conference on Multimedia Retrieval*, ICMR '19, pages 58–62, New York, NY, USA. ACM.

van der Maaten, L. and Hinton, G. (2008). Visualizing data using t-SNE. *Journal of Machine Learning Research*, 9:2579–2605.

Wang, D., Cui, P., and Zhu, W. (2016). Structural deep network embedding. In *Proceedings of the 22Nd ACM SIGKDD International Conference on Knowledge Discovery and Data Mining*, KDD '16, pages 1225–1234, New York, NY, USA. ACM.

Zafarani, R. and Liu, H. (2009). Social computing data repository at ASU.

Zhong, Z., Zheng, L., Cao, D., and Li, S. (2017). Re-ranking person re-identification with k-reciprocal encoding. In *IEEE Conference on Computer Vision and Pattern Recognition, CVPR*, pages 3652–3661.